A numerical study of axisymmetric flow regimes in a rotating annulus with local convective forcing

Susan Wright, Sylvie Su, Hélène Scolan, Roland Young and Peter Read

Atmospheric, Oceanic & Planetary Physics,
University of Oxford
peter.read@physics.ox.ac.uk

Abstract

We present a numerical study of 2D axisymmetric flows in a rotating annulus convectively forced by local thermal forcing via a heated annular ring at the bottom near the external wall and a cooled circular disk near the centre at the top surface of the annulus. Two vertically and horizontally displaced heat sources/sinks are arranged so thatstatically unstable Rayleigh-Bénard convection would be induced above the source and beneath the sink, emulating local vigorous convection in the tropics and polar regions in the Earth's atmosphere or oceans with a stably-stratified baroclinically unstable zone in mid-channel. Several distinct flow regimes are identified and characterized with reference to variations in the (squared) ratio P of Ekman layer thickness to the thermal boundary layer thickness (proportional to rotation rate Ω). Corresponding scalings for quantities such as azimuthal velocity and Nusselt number with P are consistent with convective transfer $\sim \mathrm{Ra}^{0.329\pm0.018}$ and control of meridional transport by Ekman layers in rotating flow.

1 Introduction

Complex interactions between turbulent convection and stably-stratified flows in the presence of background rotation play major roles in a wide range of problems in atmospheric and oceanic science, astrophysics and industrial flows. If a heat source is located at a lower geopotential than the sink, Sandström's theorem (Coman et al., 2006) would lead one to expect a strong, thermally-direct circulation to result. In the atmosphere of the rotating Earth, however, a situation prevails where heat sources and sinks are displaced horizontally as well as vertically, in which heating is located equatorwards and near the surface, due to the absorption of sunlight near the ground in the tropics and subsequent emission and re-absorption by the atmosphere of upwardly re-radiated thermal emission, and cooling from above by net thermal emission, predominantly at high altitude in mid-high latitudes [e.g. see Chan and Nigam (2009) and references therein]. The resulting circulation spontaneously partitions itself into a convectively unstable/neutral region in the tropics that interacts with a baroclinic region at mid-latitudes that, despite being cooled from above, is statically stable.

The mechanisms behind the formation of this statically stable region in mid-latitudes are only partially understood quantitatively, despite the apparent ability of numerical climate models to reproduce it in simulations. This lack of detailed understanding is due in part to the inability of such models to represent small-scale convection explicitly, requiring the use of parameterization methods that are empirically calibrated or 'tuned to reproduce the observed structures. But in particular, there is no well established, objective theory to account for the magnitude of the vertical thermal gradient in the mid-latitude atmosphere, although there is an ongoing debate among climate scientists as to the possible role of fully developed, baroclinic instabilities in acting to stabilise their own thermal environment [e.g. see Schneider (2006); Zurita-Gotor and Lindzen (2007)].

However, many uncertainties remain as to how such nonlinear feedbacks may arise or can be maintained in the presence of continuous radiative forcing, as well as concerning the role e.g. of moisture transports, latent heating (Juckes, 2000) and other factors.

Until recently, the most common approach to study baroclinic instability processes in the laboratory has been via the 'classical' rotating annulus experiment [e.g. see Read et al. (2014) and references therein]. In this experimental configuration, a fluid is contained between two upright, coaxial cylinders that are maintained at different temperatures, with thermally insulating horizontal or sloping endwalls. The whole assembly is then put into uniform rotation about the axis of symmetry by placing the apparatus on a rotating table. Such a configuration is not particularly well suited to address issues concerning how fully developed baroclinic instabilities interact with (and potentially control) the stratification of their environment because, with isothermal vertical walls extending across the whole depth of the tank, the latter is largely governed by intense overturning circulations in the horizontal Ekman and vertical thermal boundary layers. Baroclinic waves that develop in the interior of the experiment therefore have only a small influence on the interior stratification.

The present study aims to explore how baroclinic instabilities equilibrate in circumstances where they can exert a stronger influence on their background stratification by distributing the heat sources and sinks to avoid the formation of strong, vertical, buoyancy-dominated boundary layers. This is achieved in the present work by heating the fluid at the bottom in an annular ring near the outer cylindrical boundary and cooling via a cold plate in contact with the upper surface of the tank near the rotation axis. In this report, we present results from a set of equilibrated numerical simulations of axisymmetric circulations in a system with this set of boundary conditions and background rotation (see Scolan and Read (2016); Wright et al. (2016) for more details). Section 2 describes the configuration and model, while results are presented in Section 3 and briefly discussed in Section 4.

2 Experiment and model

The experimental configuration is illustrated in Figure 1 (right panel) in relation to its equivalent in the northern hemisphere of the Earth's atmosphere. As for the conventional rotating annulus, the fluid is contained within an annular channel between two upright, rigid, coaxial thermally insulating cylinders and a flat, horizontal base, within which the outermost 10 cm in radius is maintained at a fixed temperature T_b while for $r < b - 10$ cm the boundary is thermally insulating. The upper surface may be free-slip or (as in this case) in contact with a (non-slip) rigid lid, and thermally insulating except for the innermost $r \leq 9.25$ cm for which the temperature T_a is fixed and $T_b > T_a$. The whole system is rotating uniformly about the axis of symmetry at angular velocity Ω and the values and ranges of the main parameters are as listed in Table 1.

2.1 Numerical model

The numerical simulations in this study were undertaken using the Met. Office/Oxford Rotating Annulus Laboratory Simulation (MORALS) model (Hignett et al., 1985; Read et al., 2000), which is a finite-difference DNS code that solves the Boussinesq Navier-Stokes equations for an incompressible fluid in cylindrical annular geometry in a rotating frame of reference. The velocity boundary conditions are non-slip everywhere, i.e. $\mathbf{u} = 0$

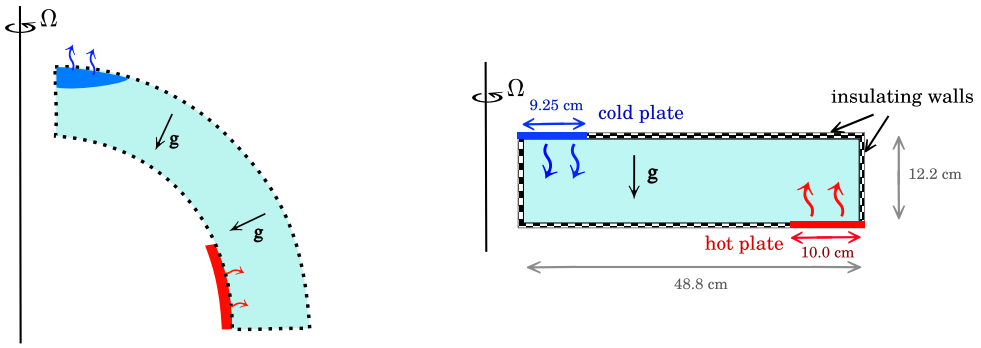

Figure 1: Configuration of the experiment (right) in radius-height cross-section, compared with its analogue (left) in a hemisphere of the Earth's atmosphere.

at the boundaries. This differs from the corresponding laboratory experiment under construction, where the top of the cylinder is a free surface. The temperature difference between the heat source and heat sink, $\Delta T = T_b - T_a$, is prescribed, and all other walls are insulating i.e. $\partial T/\partial \hat{\mathbf{n}} = 0$, where $\hat{\mathbf{n}}$ is the unit normal vector to the boundary. The pressure gradient across all surfaces is also zero. To ensure adequate resolution of the boundary layers, an Arakawa C grid which is stretched in r and z is used with 3 grid points lying within the thinner of the thermal and kinetic boundary layers. All simulations contain 384 grid points in the radial direction but the number in the vertical direction scales with height. For simulations with fluid height $d = 12.2$ cm there are 96 grid points in the z direction and 192 and 288 respectively for simulations of height 24.4 cm and 36.6 cm.

Table 1: The main parameters of the differentially heated rotating annulus experiment.

Parameter	**Symbol**	**Present range**	**Units**
Rotation rate	Ω	0–2	rad s^{-1}
Temperature difference	T	0.5–10	K
Fluid properties:			
Density	ρ	1041–1045	kg m^{-3}
Thermal expansion coefficient (at 20° C)	α_V	2.75×10^{-4}	K^{-1}
Kinematic viscosity (at 20° C)	ν	1.71×10^{-6}	m^2 s^{-1}
Thermal diffusivity (at 20° C)	κ	1.28×10^{-7}	m^2 s^{-1}
Channel geometry:			
Inner radius	a	0.025	m
Outer radius	b	0.488	m
Mean fluid depth	d	0.122, 0.244, 0.366	m
Non-dimensional:			
Ekman number (equation (1))	E	$> 6 \times 10^{-6}$	
Thermal Rossby number (equation (2))	Θ	$> 4 \times 10^{-4}$	
Prandtl number (equation (3))	σ	13.4	
Rayleigh number (equation (5))	Ra	1.1×10^7 – 3.1×10^8	
Aspect ratio (equation (4))	Γ	3.8, 1.89, 1.27	

The model was initialised with an isothermal ($T = 20°$ C) stationary fluid. The thermal and rotational forcing were applied which initially resulted in a transient regime

until the stabilisation time where the model reached equilibrium. A timestep of 0.01 s was used and most simulations were run for a total time of 50000 s. In equilibrium the total heating power into the fluid from the heat source should equal that leaving through the heat sink, as all other boundaries are insulating; this was used as a diagnostic to check when the runs had equilibrated. Simulations were computed over a range of rotation rates, temperature differences and aspect ratios. The parameters for the runs are listed in Table 1.

2.2 Dimensionless parameters

In common with the conventional rotating annulus experiment, the principal dimensionless parameters expected to govern the behaviour of the system are, the Ekman number,

$$E = \frac{\nu}{\Omega d^2}, \tag{1}$$

a stability parameter or thermal Rossby number,

$$\Theta = \frac{g\alpha_V (T_b - T_a) d}{\Omega^2 (b-a)^2}, \tag{2}$$

the Prandtl number,

$$\sigma = \frac{\nu}{\kappa}, \tag{3}$$

and the aspect ratio,

$$\Gamma = \frac{(b-a)}{d}, \tag{4}$$

where symbols are as defined in Table 1. In ordering the quantitative results on heat and momentum transport and thermal structure, we follow Hignett et al. (1981); Read (1986) and Read et al. (2014) and anticipate that a significant parameter will be the squared ratio of the characteristic length scales of the buoyancy-driven thermal boundary layer (without rotation) and Ekman layers. Assuming that the thermal boundary layer length scale $\ell_T \propto d/\mathrm{Nu} \sim d\mathrm{Ra}^{-\alpha}$, where Ra is the Rayleigh number

$$\mathrm{Ra} = \frac{g\alpha_V (T_b - T_a) d^3}{\nu\kappa}, \tag{5}$$

and α is an exponent that depends on the convective regime (e.g. see Grossmann and Lohse (2000); Chillà and Schumacher (2012)), the boundary layer ratio parameter may be defined as

$$P = \left(\frac{\ell_T}{\ell_E}\right)^2 \propto \mathrm{Ra}^{2\alpha} E^{-1}, \tag{6}$$

where $\ell_E = dE^{1/2}$ is the Ekman layer thickness; P is therefore directly proportional to Ω.

3 Results

In the following section we present results from a series of equilibrated model simulations that explore the range of axisymmetric circulations obtained in the experimental configuration described above. Key diagnostics include the Nusselt number, Nu, as a measure of the efficiency of heat transport, which is typically defined as the ratio of total heat transport through the system to that which would occur in the absence of advective transport

(i.e. due to thermal conduction alone - see Wright et al. (2016) for more details). For the present configuration with both vertically and horizontally displaced heat sources and sinks in cylindrical geometry, the conductive transport is not trivial to deduce. So this was computed here numerically from a steady state solution to the thermal diffusion equation subject to identical boundary conditions to the full problem. Nu was then computed as the ratio of the integrated heat transport by the equilibrated flow to that of the conductive solution.

3.1 Non-rotating flow

For non-rotating flow, the main issue is to determine the manner in which Nu scales with Rayleigh number. This was computed for the range $1.3 \times 10^7 < \mathrm{Ra} < 3.5 \times 10^8$ and all three values of Γ. The overall result showed a clear dependence on Ra with a value for α of 0.329 ± 0.018. This is broadly consistent with the classical result for Rayleigh-Bénard convection for $\mathrm{Nu} \propto \mathrm{Ra}^{1/3}$ (Malkus, 1954), although other values suggested for alternative convective regimes (such as 2/7) cannot be ruled out (e.g. Grossmann and Lohse, 2000; Chillà and Schumacher, 2012).

3.2 Basic phenomenology

The temperature structure of the equilibrated flow, both with and without rotation, is illustrated across a wide range of parameters in Figure 2, which shows r, z cross-sections of temperature for a range of values of P at $\Delta T = 0.5$K. This indicates several quite different regimes of convection, depending upon the relative importance of rotation in inhibiting convection and affecting the large-scale overturning circulation.

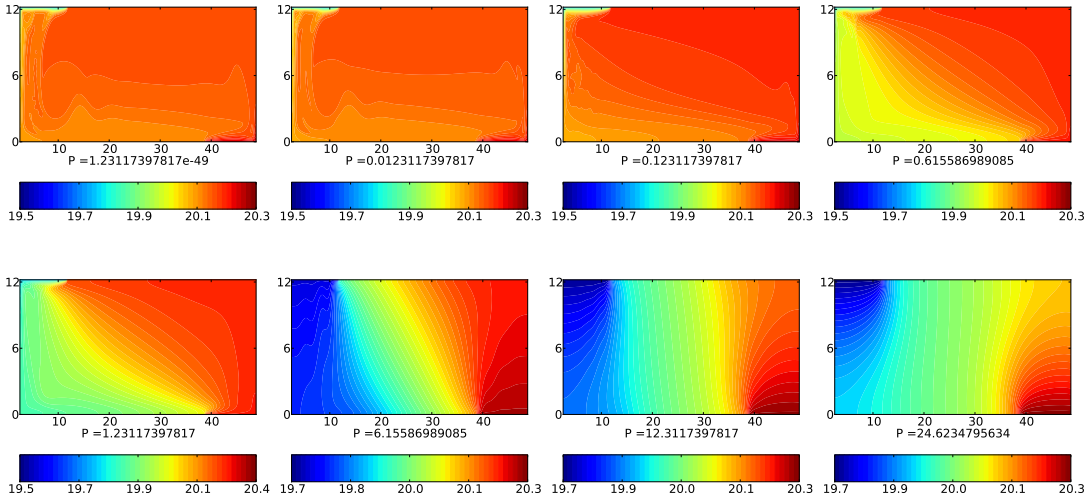

Figure 2: r, z cross-sections of the equilibrated temperature field for the full range of boundary layer parameter P (from 0 to $P \simeq 25$) at $\Delta T = 0.5$ K and varying rotation rate Ω. Colour shading represent $T - T_a$, normalised by ΔT.

In the absence of rotation, the thermal structure indicates that an axisymmetric density current descends from the heat sink on the axis and flows along the horizontal boundary towards the heat source. At this set of Rayleigh numbers, the heat exchange at the heat source is found to be sufficient to terminate the boundary current, resulting in a dynamical equilibrium. The corresponding upwelling density current above the hot plate is

less obvious, however, which is presumably a reflection of the asymmetry in area between the hot and cold plates. In contrast to the cold density current, the fluid in the upper part of the tank for $r > 15$ cm becomes almost isothermal at a temperature comparable with the hot plate itself.

In the presence of rotation, the flow undergoes several transitions towards a quite different thermal structure. For $0.1 \lesssim P \lesssim 0.6$, the cold density current disappears and the thermal gradient between hot and cold plates becomes more uniformly distributed throughout the tank. Isotherms adopt a reasonably uniform slope from top left to bottom right except close to the inner and outer boundaries, where isotherms become vertically oriented in a layer consistent with confinement to a Stewartson-like boundary layer of thickness ~ 1 cm. At larger values ($0.6 \lesssim P \lesssim 3$), near-isothermal regions develop that are aligned vertically with the hot and cold plates with a strongly baroclinic zone at intermediate radii, indicating vigorous convective mixing above the hot plate and beneath the cold plate. At the highest values of P ($P \gtrsim 5$), however, this convective mixing becomes inhibited, leading to unstably stratified thermal gradients above and below the hot and cold plates, while the isotherm slopes in the baroclinic zones become much steeper as P increases. This indicates that the flow is relaxing towards the fully conductive state as convection and overturning is inhibited by rotation, with a corresponding reduction in the static stability in the baroclinic zone.

3.3 Nusselt and velocity scaling

The influence of rotation on the circulation can be further quantified with respect to the boundary layer ratio, P, in a similar way to the work of Hignett et al. (1981); Read (1986); King et al. (2012); Read et al. (2014) and others for various problems in rotating convection. Figure 3(a) shows the variation with P of a scaled Nusselt number, (Nu-1)/Nu_0, where Nu_0 is the value of Nu at $\Omega = 0$ for the corresponding value of Ra. Figure 3(b) shows the corresponding variation of the azimuthal velocity scale

$$\hat{V} = \frac{< V > (b-a)}{\kappa \Gamma \mathrm{Nu}_0^2}, \tag{7}$$

where $\mathrm{Nu}_0 \sim \mathrm{Ra}^{\alpha}$ and $< V >$ is a measure of the mean azimuthal velocity, for the three different aspect ratios.

Fig. 3(a) clearly demonstrates that rotation has little effect on heat transport until $P \gtrsim 1-10$, beyond which the advective part of Nu (= Nu - 1 $\sim$ Péclet number) decreases as $P^{-3/2}$, though with some dependence on aspect ratio. The corresponding behaviour of $\hat{V}$ shows the velocity scale increasing almost linearly with P at very low rotation rates, peaking around $P \sim O(1)$ and then decreasing roughly as P^{-1} for $P >> 1$. This suggests the existence of a number of distinct axisymmetric regimes along similar lines to those found in the classical rotating annulus (Hignett, 1982; Read et al., 2014), indicating a critical role for the Ekman layers in controlling advective heat transfer when their thickness becomes comparable to or thinner than the thermal boundary layers. The linear dependence of $\hat{V}$ on P and Ω at very low rotation rates indicates an angular momentum quasi-conserving regime (regime (ii) of Hignett (1982); Read et al. (2014)), while its dependence as P^{-1} at high values of Ω is consistent with the thermal wind shear relation for geostrophic flow at constant isotherm slope (regime (v) of Hignett (1982); Read et al. (2014)). This is also consistent with the $P^{-3/2}$ dependence of Nu-1 in a regime dominated by Ekman transport, for which mass flow in an Ekman layer $\propto \hat{V}\ell_E \sim \Omega^{-3/2}$ (Hignett,

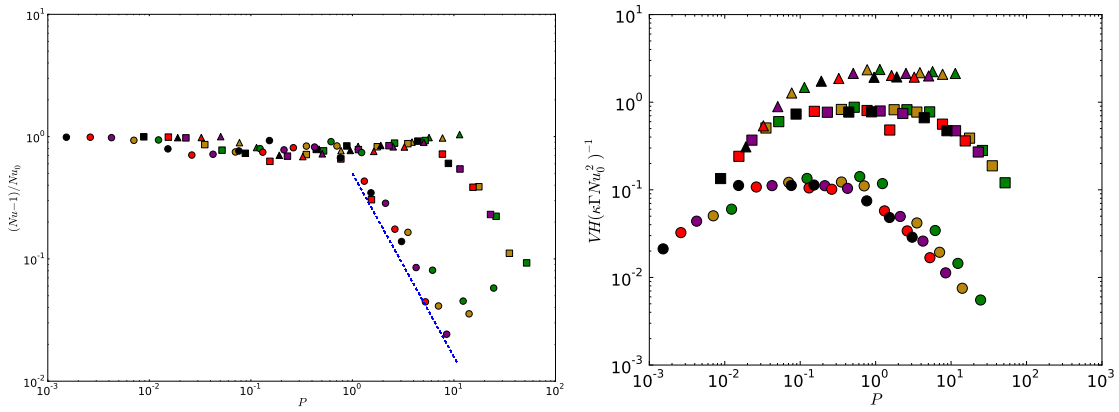

Figure 3: (a) The reduced Nusselt number (Nu-1)Nu_0^{-1} (where Nu_0 is the value of Nu without rotation) and (b) zonal velocity scale, scaled following Read (1986); Read et al. (2014), as a function of boundary layer parameter P. The dashed line in (a) has a slope of -3/2, corresponding to the rotationally dominated regime (v) discussed e.g. by Read et al. (2014). Circles represent $\Gamma = 3.8$, squares for $\Gamma = 1.89$ and triangles for $\Gamma = 1.27$.

1982; Read et al., 2014). In between these regimes, the dependence of $\hat{V}$ with P levels off, varying either as $P^{1/2}$ for $\sigma^{-2} < P < 1$ (regime (iii)) or becoming independent of P for $P \sim O(1)$ (regime (iv)).

4 Discussion

This study has explored and identified a number of distinct axisymmetric circulation regimes in a novel experimental configuration that combines statically unstable convection with large-scale overturning. The resulting flows include cases in which a stably-stratified baroclinic zone, with sloping isopycnals and isotherms, is obtained between two convectively unstable regions adjacent to the laterally displaced heat source and sink. Such a situation evidently occurs within analogues of the regimes (iii) - (v) of Hignett (1982); Read (1986) and Read et al. (2014). Experience of similar regimes in the classical rotating annulus would suggest that vigorous baroclinic instability is likely to occur under conditions consistent with regimes (iv) and (v), and so conditions for which $P \gtrsim 1$ should provide an appropriate context in which to explore the equilibration of baroclinic instability and possible effects of 'baroclinic adjustment' (Schneider, 2006; Zurita-Gotor and Lindzen, 2007) in future experimental studies (see the contribution in this volume by Scolan et al.) and fully 3D numerical simulations. Further work is needed, however, to elucidate in more detail the nature of convection in this system and its partitioning between boundary layers and the interior e.g. in the context of Grossmann-Lohse theory or alternative hypotheses. The quantitative dependence of flow properties on the aspect ratio Γ is also not fully understood for this system and should receive further attention in future studies. This work was supported by UK EPSRC grant EP/K029428/1 and the Oxford/Met Office Academic Partnership.

References

Chan, S. C. and Nigam, S. (2009). Residual diagnosis of diabatic heating from ERA-40 and NCEP reanalyses, intercomparisons with TRMM. *J. Clim.*, 22:414–428.

Chillà, F. and Schumacher, J. (2012). New perspectives in turbulent Rayleigh-Bénard convection. *Eur. Phys. J. E*, 35:58.

Coman, M. A., Griffiths, R. W., and Hughes, G. O. (2006). Sandström's experiments revisited. *J. Mar. Res.*, 64:783–796.

Grossmann, S. and Lohse, D. (2000). Scaling in thermal convection: A unifying theory. *J. Fluid Mech.*, 407:27–56.

Hignett, P. (1982). A note on the heat transfer by the axisymmetric thermal convection in a rotating fluid annulus. *Geophys. Astrophys. Fluid Dyn.*, 19:293–299.

Hignett, P., Ibbetson, A., and Killworth, P. D. (1981). On rotating thermal convection driven by non-uniform heating from below. *J. Fluid Mech.*, 109:161–187.

Hignett, P., White, A. A., Carter, R. D., Jackson, W. D. N., and Small, R. M. (1985). A comparison of laboratory measurements and numerical simulations of baroclinic wave flows in a rotating cylindrical annulus. *Q. J. R. Meteorol. Soc.*, 111:131–154.

Juckes, M. N. (2000). The static stability of the midlatitude troposphere: the relevance of moisture. *J. Atmos. Sci.*, 57:3050–3057.

King, E. M., Stellmach, S., and Aurnou, J. M. (2012). Heat transfer by rapidly rotating Rayleigh-Bénard convection. *J. Fluid Mech.*, 691:568–582.

Malkus, W. V. R. (1954). The heat transport and spectrum of thermal turbulence. *Proc. R. Soc. London, Ser. A*, 225:196–212.

Read, P. L. (1986). Regimes of axisymmetric flow in an internally heated rotating fluid. *J . Fluid Mech*, 168:255–289.

Read, P. L., Pérez, E. P., Moroz, I. M., and Young, R. M. B. (2014). General Circulation of Planetary Atmospheres: Insights from Rotating Annulus and Related Experiments. In von Larcher, T. and Williams, P. D., editors, *Modeling Atmospheric and Oceanic Flows: Insights from Laboratory Experiments and Numerical Simulations*, pages 7–44. American Geophysical Union.

Read, P. L., Thomas, N. P. J., and Risch, S. H. (2000). An evaluation of Eulerian and Semi-Lagrangian advection schemes in simulations of rotating, stratified flows in the laboratory. part I: Axisymmetric flow. *Mon. Wea. Rev.*, 128:2835–2852.

Schneider, T. (2006). The general circulation of the atmosphere. *Annu. Rev. Earth Planet. Sci.*, 34:655–688.

Scolan, H. and Read, P. L. (2016). Convectively forced thermally-driven rotating annulus: a new atmosphere-like experiment. *Expt. in Fluids*, in preparation.

Wright, S., Su, S., Scolan, H., Young, R. M. B., and Read, P. L. (2016). Regimes of axisymmetric flow and scaling laws in a rotating annulus with local convective forcing. *J. Fluid Mech.*, in preparation.

Zurita-Gotor, P. and Lindzen, R. S. (2007). Theories of baroclinic adjustment and eddy equilibration. In Schneider, T. and Sobel, A. H., editors, *The Global Circulation of the Atmosphere*, pages 1–21. Princeton University Press, Princeton, USA.